Multimedia Tools and Applications
https://doi.org/10.1007/s11042-018-6424-4

Rich club characteristics of dynamic brain functional networks in resting state

Zhuqing Jiao[1] · Huan Wang[1] · Min Cai[1] · Yin Cao[2] · Ling Zou[1] · Shuihua Wang[3]

Received: 1 June 2018 / Revised: 26 June 2018 / Accepted: 18 July 2018
Published online: 25 July 2018

Abstract

Conventional brain functional networks are constructed by extracting the entire time series from functional Magnetic Resonance Imaging (fMRI). Yet such a method is easy to ignore the dynamic interaction patterns of brain regions that essentially change across time. In this study, we analyze the functional connectivity characteristics of Rich Club in resting-state brain functional networks, and study the dynamic functional differences of core brain regions at different time periods. First, the time series is extracted from resting-state fMRI to construct a dynamic brain functional network. Then, Rich Clubs of different time periods are determined by the Rich Club coefficients. In particular, the efficiency of each Rich Club is calculated to examine the influences of the Rich Connections, Feeder Connections and Local Connections. Finally, the node degree, clustering coefficient and efficiency for Rich Club nodes are calculated to quantify the dynamic processes of Rich Clubs, and the functional connectivity of Rich Clubs are compared with those of the functional networks constructed by the entire fMRI time series. Experimental results demonstrate that the distribution of Rich Clubs in the dynamic brain functional network is consistent with that from the entire fMRI time series, while the composition and functional connectivity of Rich Club dynamically change across time. Moreover, Rich connection and Local connection in the brain functional networks show a significant correlation with the efficiency of Rich Club, and the local and the global efficiency of Rich Clubs are greater than that of the global network. These results further illustrate the viewpoint that Rich Clubs have significant influence on the functional characteristics of global brain functional networks.

Keywords Functional magnetic resonance imaging (fMRI) · Time series · Brain functional networks · Rich club

✉ Ling Zou
zouling@cczu.edu.cn

✉ Shuihua Wang
shuihuawang@ieee.org

Extended author information available on the last page of the article

1 Introduction

Deep learning reorganizes data by imitating human's way of thinking to get the higher dimensional and abstract features of things [45]. A noticeable application of current deep learning is on medical image recognition, for example, the analysis of functional Magnetic Resonance Imaging (fMRI) using deep Convolutional Neural Networks (CNN) models [40, 41, 55]. Specifically, many scientists have applied deep learning to computer-aided medical diagnosis. However, obtaining effective feature data is an important prerequisite for deep learning. The human brain is an extremely complex system that exists in nature. Its neuronal cells are linked together by synapses, forming a very complex brain structure network that is the structural basis for the brain to perform a variety of physiological and cognitive activities [8, 29]. Brain network topologies of patients with neuropsychiatric and neurological diseases show significant differences compared with normal person. Recently, the researches of the brain networks have drawn much attention and made good progress [16]. However, there is no definite conclusion so far on the organizational pattern mode that leads to the abnormal connection of nodes in brain networks, which have yet to be further studied.

In modern medicine, a brain can be structured in several functional partitions. If regarding different functional partitions as the corresponding nodes, the connection between functional partitions can be abstracted into a link between two nodes [17]. As a result, all of these nodes and edges will make up a brain functional network, which is similar to many other complex networks [18, 30]. Some nodes with larger degree in brain networks play an essential role in the overall function of the network, and the connection densities between the nodes are greater than those between the nodes with smaller degree. Therefore, there is a phenomenon that the connections are highly dense in some local areas. Besides, the module has the characteristics with shorter path length and a smaller degree of aggregation, which is called Rich Club [12, 24, 26].

The constituent nodes in the Rich Club are called Rich Club nodes. This kind of node integrates the various functional modules of the brain through its high connection, and forms the core structure of the whole brain functional network, which plays an important role in the interaction and integration of information [6, 23, 43]. Core nodes are very difficult to withstand the attack of diseases compared with the general nodes because of high participation in brain functional activities. Moreover, dysfunction of core brain regions can be expected to result in the disorder of the connection for the global brain network or local network [11, 19, 34, 48]. The topologies of Rich Clubs have obvious exceptions in the brain functional networks of the patients with mental or neurological diseases. Thus, topological properties of Rich Club in brain functional network can contribute to understand the pathological mechanism of brain diseases on brain functional networks, and deepen the understanding of abnormal brain functions [13, 31].

Conventional studies on functional connectivity generally assume that the brain activity is in a stable state at different times, and the functional connectivity between brain regions or voxels is quantified through a network model constructed from the fMRI time series of brain regions [15, 46, 49, 51]. This actually implicitly hypothesizes the stationary interaction patterns among brain regions. In recent years, the neural activities in brains have been found to be not always in a stable state but dynamically changes across time, and this phenomenon exists not only in the resting state but also in the task state [1, 4]. Therefore, the correlation among the entire fMRI time series simply measures the functional connectivity between brain regions with a scalar value, which is set across time. As a result, this method can overlook the complex and dynamic interaction patterns among brain regions which are essentially time-varying [2, 35, 52].

Sliding time window contributes to reveal the dynamic process of functional connectivity [25, 28]. The fMRI time series of brain regions is hereby divided into several sub-segments and the functional networks based on each sub-segment time series are introduced to analyze the functional connectivity properties of the same brain region at different time layers [7, 27]. Nowadays, great progress has been achieved in the auxiliary diagnosis of patients with brain diseases by constructing dynamic brain functional networks. Wang et al. [39] constructed a dynamic brain function network, by which the accuracy rate of classification for AD patients was 92.31%. Chen et al. [3] used the sliding time window method to construct a high-order brain functional network, and the classification accuracy reached 88.14% with early mild cognitive impairment (MCI) patients. Accordingly, studying the dynamic characteristics of brain function networks can bring a more comprehensive understanding of the functional organization mode of brains [9, 10, 47].

In this study, we take resting-state fMRI data of stroke patients as objects to research functional connectivity characteristics of Rich Clubs in dynamic brain functional networks, which are constructed based on *Pearson* correlation. Then Rich Clubs from sub-time series of different time periods are determined to compare the node composition, and the edge types and the efficiency of Rich Club with that by entire fMRI time series. In addition, we discuss the differences of Rich Club characteristics with different coefficients, especially in dynamic brain functional networks. The rest of the article is organized as follows. In Section 2, we introduce the Rich Clubs from dynamic brain functional networks. In Section 3, we describe experimental materials and analyze the respective results. In Section 4, we discuss the Rich Club characteristics of the dynamic network and that from the entire time series and conclude this research.

2 Methods

The whole brain is divided into 90 brain regions (The left and right brains are divided into 45 regions respectively) according to AAL (Automated Anatomical Labeling) standard partition template [36, 38]. After extracting fMRI time series of all brain regions, the sliding time window parcels out the entire fMRI time series of each region into several sub-segments, which overlap each other and have same window length. Finally, the *Pearson* correlation of every sub-time series of all regions is computed to construct dynamic brain functional networks. The specific steps are as follows [42]:

(1) If the length of the entire fMRI time series is M, and the number of brain regions is K ($K = 90$), so the combination of time series for all brain regions is a matrix of $M \times K$;
(2) Supposing that the length of each time window is L, the step size is s, and entire time series is divided into l segments, then l is defined as:

$$l = \frac{M-L}{s} + 1 \tag{1}$$

(3) Computing the *Pearson* correlation coefficient between the time series representing two different brain regions to obtain the correlation coefficient matrix in each window. The *Pearson* correlation coefficient r is defined as:

$$r = \frac{\sum_{i=1}^{N} (X_i - X^{--})(Y_i - Y^{--})}{\sqrt{\sum_{i=1}^{N} (X_i - X^{--})^2 \sum_{i=1}^{N} (Y_i - Y^{--})^2}} \tag{2}$$

where X_i and Y_i are the i-th elements of the time series $\boldsymbol{X}$ and $\boldsymbol{Y}$, respectively; $\overline{X}$ and $\overline{Y}$ are the means of all the elements in $\boldsymbol{X}$ and $\boldsymbol{Y}$, respectively; N is the number of the elements in each time series.

Previous studies have shown that nodes with higher degrees in the network are often connected with nodes with the same characteristics, and the module formed is also more intensive. Zhou and Mondragon [54] described the topological properties of the structure by defining a Rich Club coefficient, which represents the ratio of the actual number of connected edges between the r nodes with the highest degree of nodes to the maximum number of possible edges.

For a given network G, node i is connected to k nodes. The nodes with less than k edges are removed, and the remaining nodes form a Rich Club [37]. Actually, there are two cases: weighted and unweighted, and the unweighted Rich Club coefficient of the original network is expressed as follows:

$$\varphi(r) = \frac{2E > k}{N > k(N > k-1)} \tag{3}$$

where $N_{>k}$ represents the number of nodes whose degree is greater than k, and $E_{>k}$ represents the actual number of connected edges between these nodes.

It is noteworthy that Rich Club phenomenon exists in the network when $\varphi(r)$ increases as k increases. In random networks, Erods-Renyi model also has such a phenomenon that the nodes with higher degrees tend to be connected to the nodes with higher degrees, and $\varphi(r)$ appears to increase with the increase of k [44]. Therefore, Colizza et al. [5] thought that Rich Club exists in the real network, only when the ratio of the Rich Club coefficient in the original network to the Rich Club coefficient of the random network on the same condition is larger than 1. This ratio called the normalized Rich Club coefficient is defined as:

$$\varphi_{\text{norm}}(r) = \frac{\varphi(r)}{\varphi_{\text{rand}}(r)} \tag{4}$$

where $\varphi_{\text{rand}}(r)$ is the average of the Rich Club coefficients from a certain amount of random networks, which have not only the equal number of nodes and edges but the same degree distribution as the original network [32].

The dynamic change characteristics of Rich Clubs are analyzed according to the complex network index after determining Rich Clubs in the network [14, 20, 22]. If there are unconnected nodes in the network, the shortest path length of the network is infinite [21, 33]. Hence the shortest path length can be utilized to ensure whether a brain functional network constructed by the time series is a fully connected graph. Furthermore, the information transfer rate has a significant effect for analysis of the information transfer rate.

Suppose the number of nodes in the network G is N_G, the shortest path length l_{ij} from the node v_i to the node v_j is defined as the minimum number of edges to experience from v_i to v_j. Then the shortest path length L of the network is:

$$L = \frac{1}{NG(NG-1)} \sum_{i \neq j \in G} lij \tag{5}$$

The shorter the shortest path length between nodes, the faster the information transfer rate and the higher the information transfer efficiency, and the higher the efficiency of the global network. Hence the local information transmission capability of the network is measured by the local efficiency. In the network G, the local efficiency $E_{\mathrm{loc}}(i)$ of the node v_i is:

$$E\mathrm{loc}(i) = \frac{1}{NG(NG-1)} \sum_{i \neq j \in G} \frac{1}{lij} \tag{6}$$

The local efficiency E_{loc} of the network is the average of local efficiency of all nodes in the network:

$$E\mathrm{loc} = \frac{1}{NG} \sum_{i \in G} E\mathrm{loc}(i) \tag{7}$$

The shortest path length of the nodes can measure the global efficiency of the network. For network G, the global efficiency E_g of the network is:

$$Eg = \frac{1}{NG(NG-1)} \sum_{i \neq j, i, j \in V} lij \tag{8}$$

3 Experiments and results

Our experiments are performed in 15 stroke patients and 20 normal controls, all of which are carried on fMRI scanning in the resting state. The stroke patients include 9 males and 6 females, aged between 60~75 years old. The controls include 10 males and females, aged between 18~25 years old. The data collection process is performed at Changzhou Second People's Hospital and approved by the Ethics Committee of Changzhou University. Before acquiring brain fMRI data, we need to understand the physical condition of volunteers, and asked them to check whether there are metallic products on bodies. At the same time, reminding the participants to stay awake and do not have any conscious thinking activities.

A PHILIPS 3.0-Tesla scanner at Changzhou No.2 People's Hospital is used to locate the particular regions of the brain cortex and collect resting-state brain fMRI. Scanning parameters are set as follows. Functional Image: Axial Slices = 24, Layer Thickness = 4 mm, Repeat Time TR = 2000 ms, Echo Time TE = 35 ms, angle flip = 90°, FOV = 230 mm × 182 mm. Structure Image: 3D Sequence Number = 270, Layer Thickness = 0.6 mm, Repeat Time TR = 7.4 ms, Echo Time TE = 3.4 ms, Angle Flip = 8°, FOV = 250 mm × 250 mm.

SPM (Statistical Parametric Mapping) (http://www.fil.ion.ucl.ac.uk/spm/) and DPARSF (Data Processing Assistant for Resting-State fMRI) (http://rfmri.org/DPARSF) are used to convert and preprocess the raw data, including: time correction, spatial registration, standardization, and filtering. The filtering range is: 0.01~0.08 Hz, standardized Bounding Box: [−90, −126, −72; 90, 90, 108], Voxel Size: [3 3 3]. Due to the machine and volunteers to stabilize may take a certain amount of time, the fMRI image data for the first 15 time points is removed during processing.

One single stroke patient (Sex: Male, age: 60 Years) is randomly selected to study. The number of original fMRI images is 120, since the fMRI images data for the first 15 time points is removed, and the length of entire fMRI time series is 105. Zhang et al. [53] have discussed

the effect of window length on classification accuracy of MCI patients, and they found that the effect was best when window length was placed at 70. So the window length is also set to $L = 70$ for this research. The step size is taken in a more relaxed manner due to only research the dynamic characteristics of functional connection, and it is set to $s = 5$. According to Eq. (1), the number of sliding windows is 8. They are windows *a*, *b*, *c*, *d*, *e*, *f*, *g*, and *h*, respectively.

The *Pearson* correlation coefficient between the time series of two brain regions in all windows is calculated, and the correlation coefficient matrix is binarized by different threshold values. The shortest path length of the network constructed by each window is generated under different thresholds. The threshold starts from 0 and the step length is 0.01. The above complex network indicators are implemented in the Brain Connectivity Toolbox (BCT) (https://www.nitrc.org/projects/bct/) [32].

Table 1 shows the properties of the brain functional networks, constructed by the fMRI time series segments of all brain regions from windows *a*, *c*. The threshold chosen is the smallest among all windows when the shortest path length of the network is infinite. Then the network density of window *a* is up to 33.52%. The network density is supposed to be 35% to ensure that all windows have uniform network density. Consequently, the window thresholds of $a \sim h$ are: 0.37, 0.37, 0.36, 0.36, 0.36, 0.37, 0.38, and 0.39, respectively. Moreover, the threshold of all windows has a small range of change. It indicates there are no dramatic changes in the overall functional connectivity between all nodes in the network. The GRETNA toolbox (https://www.nitrc.org/projects/gretna) is carried out to calculate the Rich Club coefficients of the network for each window. Then 1000 random networks corresponding to the windows with the same number of nodes, edges and degree distribution are constructed according to the original network, and the average values of the Rich Club coefficients in these random networks are calculated.

According to the definition of Rich Club, it is considered that the Rich Club module exists in the network if the Rich Club coefficient of the original network and the Rich Club coefficient of the corresponding random network increase with the number of nodes *k*, and the normalized Rich Club coefficient is greater than 1. Figure 1 shows the Rich Club coefficients of the functional networks from windows *a* to *h* with a range of *k*, for $\varphi(r)$ (dark), $\varphi_{rand}(r)$ (red) and $\varphi_{norm}(r)$ (blue). $\varphi_{norm}(r)$ is found to be larger than $\varphi_{rand}(r)$, suggesting rich-club organization for all eight windows of the brain functional network. Especially, these figures show an increasing normalized rich-club coefficient $\varphi_{norm}(r)$ for a range of *k* from 9 to 21. Thus it can be observed that, there are significant differences in the ranges of their minimum node degree when the Rich Club phenomenon appears in the brain functional network constructed by different windows. Meanwhile, the Rich-

Table 1 Properties of brain functional network in different time windows

Sliding windows	Critical threshold	Shortest path length of network	Network density	The number of edges
a	0.38	2.4120	33.52%	657
b	0.41	2.6005	29.49%	578
c	0.38	2.5009	32.50%	637
d	0.48	3.1588	20.22%	397
e	0.48	3.2242	21.58%	417
f	0.48	3.1838	22.94%	440
g	0.49	3.3710	22.73%	439
h	0.51	3.4537	21.57%	424

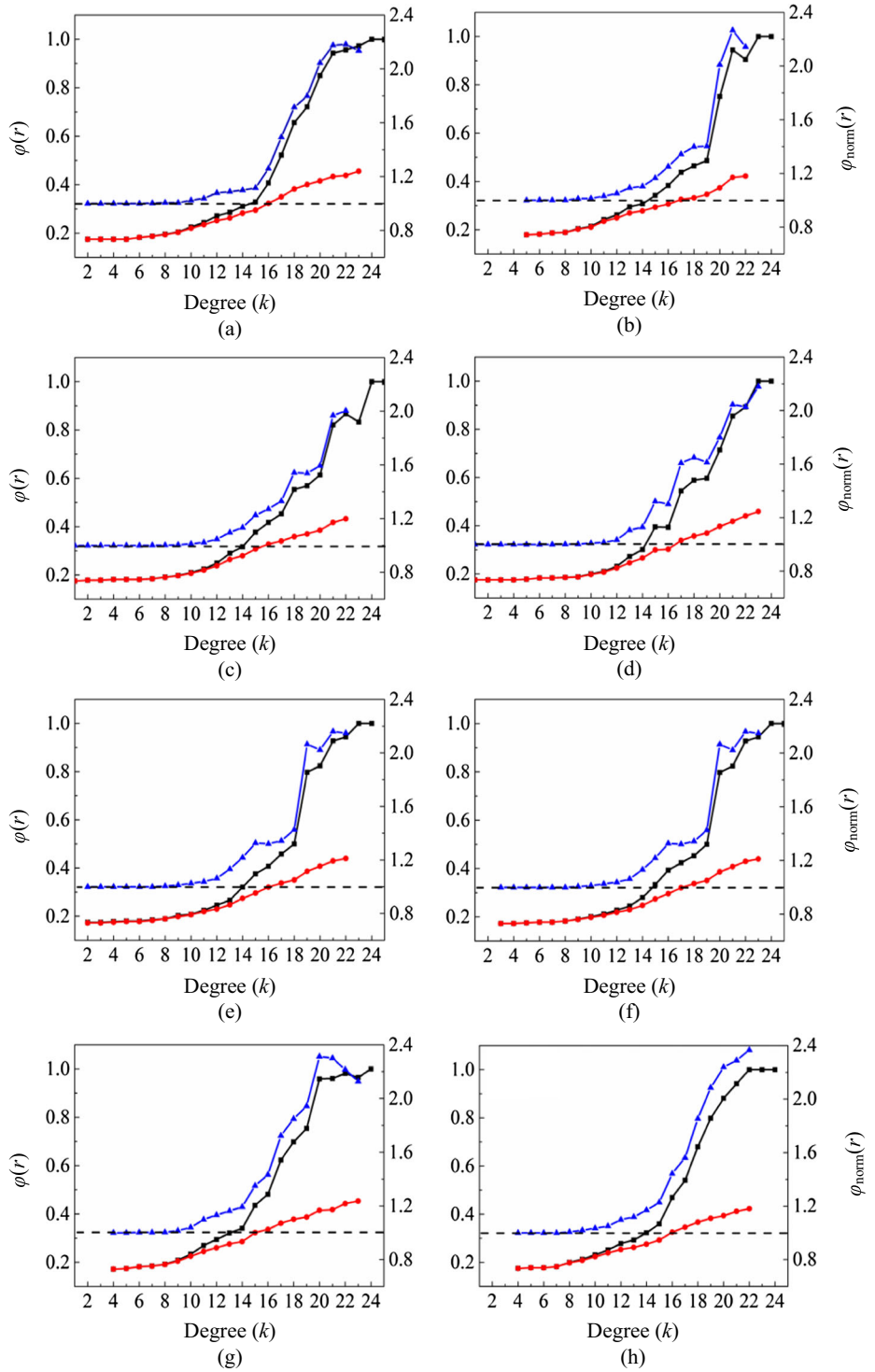

Fig. 1 Rich Club coefficients of functional networks from windows *a* to *h*

Club behavior of the functional network indicates that temporal changes have occurred in the functional connection between nodes.

The Rich Club with significant difference between the original network and the random network is selected, and the structure when the normalized Rich Club coefficient reaches the maximum value is analyzed. Table 2 shows all the nodes of the Rich Clubs and their ranges and numbers in the windows *a* to *h* according to node degree.

As seen from Table 2, the composition of Rich Club at different time periods is different, which means functional connection among Rich Club nodes is also dynamically changing. Although the number of nodes and connections are constantly changing, some nodes always appear in different Rich Club modules. For example, all nodes of window d appeared in other Rich Club modules, it shown that these nodes are always in a more active state. The software BrainNet Viewer (https://www.nitrc.org/projects/bnv/) is used to visualize Rich Club for each window instead of describing the connection relationship of nodes from adjacency matrix. Figure 2 shows the functional connectivity of Rich Clubs for the windows *a* to *h*.

Combining with Table 2 and Fig. 2, the distribution and composition of Rich Club in each window is very different, and the functional connectivity has changed significantly. In particular, the Rich Club of window *d* has fewer nodes and sparser connection density. The numbers of different types of connections at different time periods are computing. Among them the rich connection is a connection between Rich Club nodes, the feeder connection is a connection between non-Rich Club node and Rich Club node, and the local connection is a connection between non-Rich Club nodes. Table 3 shows the proportion of different types of edges in the network,

As seen from Table 3, it can be seen that the ratios of various types of edges in all network are quite different in different time windows. Since Rich Club nodes have a high connection density, which connects the larger brain regions together, the module may play an essential role in the processing and transmission of information. To analyze the information transfer

Table 2 The nodes composition of Rich Clubs in different window networks

Sliding windows	Degree range	Number of nodes	Composition of rich club Abbr (L: Left R: Right)
a	$k \geq 22$	15	IFGoperc.R, HIP.R, PHG.R, IOG.R, FFG.R, PoCG.R, IPL.R, SMG.R, ANG.R, PUT.R, HES.R, STG.R, TPOsup.R, MTG.R, ITG.R
b	$k \geq 21$	18	IFGoperc.R, ROL.R, HIP.R, PHG.R, AMYG.R, CUN.R, MOG.R, IOG.R, FFG.R, PoCG.R, IPL.R, SMG.R, ANG.R, PUT.R, HES.R, TPOsup.R, MTG.R, ITG.R
c	$k \geq 22$	13	ROL.R, HIP.R, PHG.R, CUN.R, LING.R, IOG.R, FFG.R, PoCG.R, IPL.R, PUT.R, HES.R, TPOsup.R, ITG.R
d	$k \geq 23$	8	HIP.R, FFG.R, PoCG.R, IPL.R, ANG.R, HES.R, TPOsup.R, ITG.R
e	$k \geq 21$	14	ROL.R, HIP.R, CAL.R, FFG.R, PoCG.R, IPL.R, SMG.R, ANG.R, PUT.R, HES.R, STG.R, TPOsup.R, MTG.R, ITG.R
f	$k \geq 22$	14	ROL.R, HIP.R, PHG.R, FFG.R, PoCG.R, IPL.R, SMG.R, ANG.R, PUT.R, HES.R, STG.R, TPOsup.R, MTG.R, ITG.R
g	$k \geq 20$	24	PreCG.R, MFG.R, IFGoperc.R, IFGtriang.R, ORBinf.R, ROL.R, HIP.R, PHG.R, AMYG.R, CUN.R, SOG.R, FFG.R, PoCG.R, SPG.R, IPL.R, SMG.R, ANG.R, PUT.R, HES.R, STG.R, TPOsup.R, MTG.R, TPOmid.R, ITG.R
h	$k \geq 22$	16	PreCG.R, IFGoperc.R, ORBinf.R, ROL.R, HIP.R, PHG.R, FFG.R, PoCG.R, SPG.R, IPL.R, ANG.R, HES.R, STG.R, MTG.R, TPOmid.R, ITG.R

The name of the brain regions in the table is AAL standard partition template abbreviated

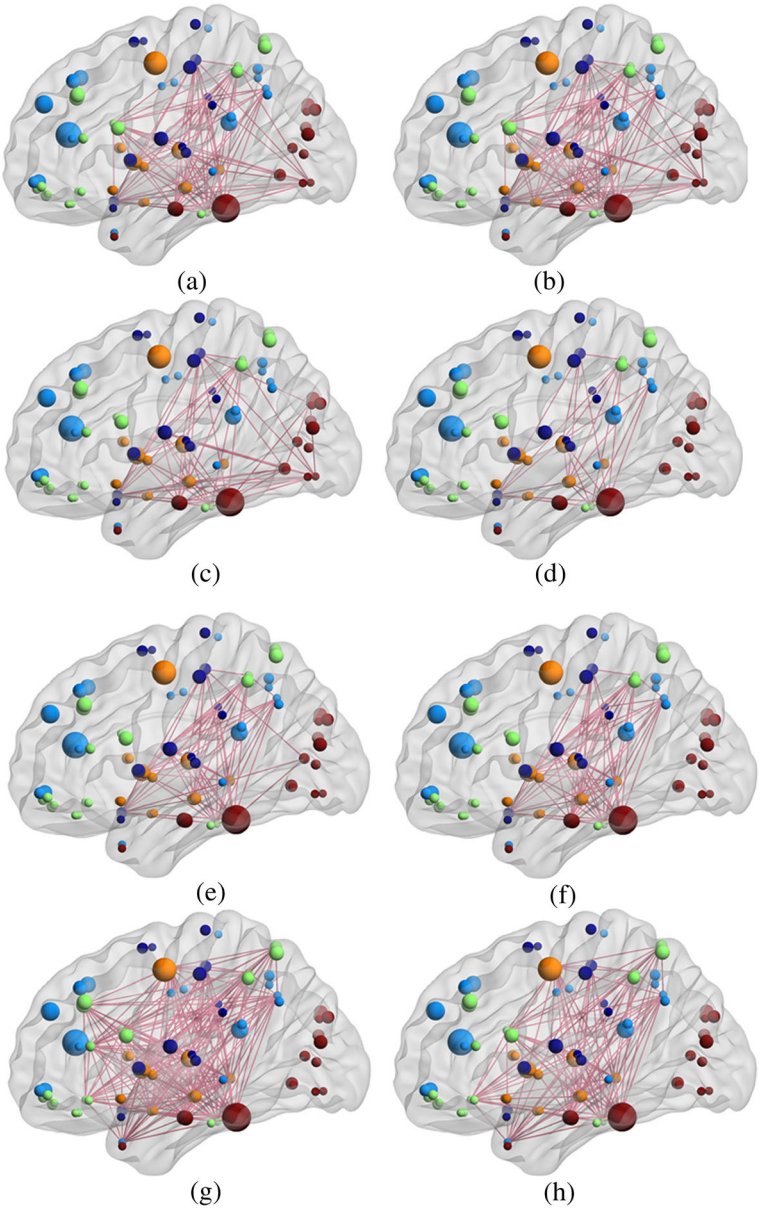

Fig. 2 Functional connectivity of Rich Clubs for window *a* to *h*

efficiency for brain functional network and Rich Club, the global efficiency and local efficiency of them for each window are calculated, as shown in Fig. 3.

It appears in Fig. 3 that the global efficiency and local efficiency of the brain functional network for the stroke patient are less than those of Rich Club, while the information transmission rate in brain functional network is lower than that of Rich Club. The local efficiency of the brain functional network and Rich Club is higher than the global efficiency, and the efficiency has a certain range of fluctuations in different time windows.

Table 3 The proportion of different types of edges

Sliding windows	Rich connections (%)	Feeder connections (%)	Local connections (%)	Edges
a	14.43	23.91	61.66	686
b	16.76	24.93	58.31	686
c	9.33	26.38	64.29	686
d	3.64	21.4	74.96	687
e	11.08	26	62.92	677
f	12.52	24.44	63.04	671
g	30.77	18.49	50.74	676
h	16.42	21.37	62.21	688

Although the node composition and node activity of Rich Club in the network change at different time, the module is always at the core of the brain functional network. In addition, the effects of different kinds of edge on global efficiency and local efficiency of Rich Club are statistically analyzed by using Statistical Product and Service Solutions (SPSS) software. The results are shown in Table 4.

According to Table 4, Rich connection and Local connection have significant correlation with the global efficiency and local efficiency of Rich Club in the functional networks from different fMRI time series sub-segments. There are considerable negative correlations, not only between the Rich connection and the local efficiency but between the Local connection and the global efficiency. The Rich connection and the global efficiency, as well as the Local connection and the local efficiency, have a significant positive correlation while the Feeder connection has no significant correlation with the Rich Club efficiency. It just means that the influence of different types of edges on Rich Club efficiency is statistically significant, and does not represent the strength of the actual structure.

4 Discussion

In order to be consistent with dynamic brain function networks, a functional network of brain is constructed by using fMRI sequence of all brain regions. The selected network density is

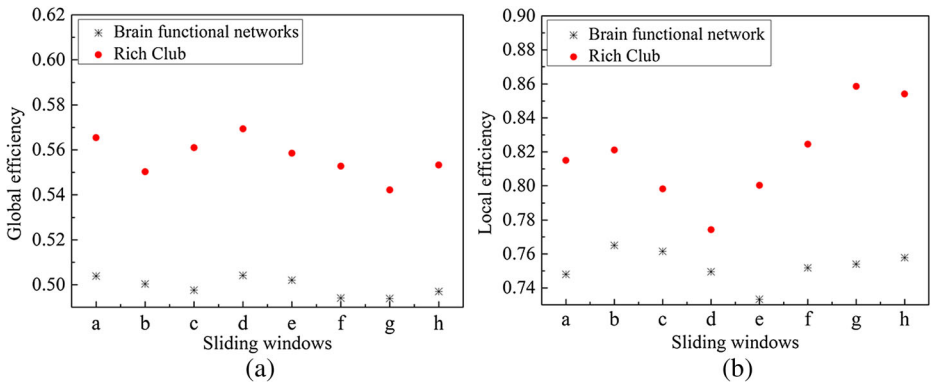

Fig. 3 The efficiencies of global network and Rich Club. **a** The global efficiency of global network and Rich Club. **b** The local efficiency of global network and Rich Club

Table 4 Statistical results of the correlation between different kinds of edge and efficiency

Network	Efficiency	Rich connections	Feeder connections	Local connections
Rich Club	Local efficiency	$r = -0.8622$ $P = 0.0059^*$	$r = 0.3659$ $P = 0.3726$	$r = 0.8634$ $P = 0.0057^*$
	Global efficiency	$r = 0.8718$ $P = 0.0048^*$	$r = -0.5203$ $P = 0.1862$	$r = -0.8124$ $P = 0.0143^*$

r in the table indicates correlation; * indicates $P < 0.05$

still 35%, and the threshold is 0.36. Accordingly, the shortest path length of the network is 2.4235, and all nodes constitute a fully connected graph. On this basis, the Rich Club coefficient of the brain functional network is calculated and the degree distribution corresponding to the original network is constructed by the 1000 random networks with the same number of nodes and edges. As a result, The average values of the Rich Club coefficients are obtained for these random networks. Figure 4 shows the Rich Club coefficients of the brain function network in the brain of the stroke patient.

In Fig. 4, $\varphi_{norm}(r)$ (blue) is larger than $\varphi_{rand}(r)$ (red) and $\varphi(r)$ (dark) for a range of k. Accordingly, when the typical Rich Club phenomenon occurs in brain functional network of stroke patient with entire fMRI time series, the range of the minimum node degree is in 9 to 21 in the module consisting of a few nodes with the largest degree. The most significant Rich Club module is selected for analysis, by which is the normalized Rich Club coefficient reaches the maximum value. The minimum degree of the node that consists of Rich Club is 21. Figure 5 shows the degrees of all nodes of brain functional network in stroke patients. The corresponding brain regions from Label 1 to Label 90 contribute to determine the composition of Rich Clubs.

Table 5 shows the node composition of Rich Club in the brain functional network based on node degree.

The spatial distribution of Rich Club in the brain functional network constructed by entire fMRI time series is consistent with that in the dynamic brain functional network at aspects of composing the structure. Comparing Tables 2 and Table 5, it is evident that the Rich Club nodes in window d are all part of the Rich Club in other windows, which indicate that the

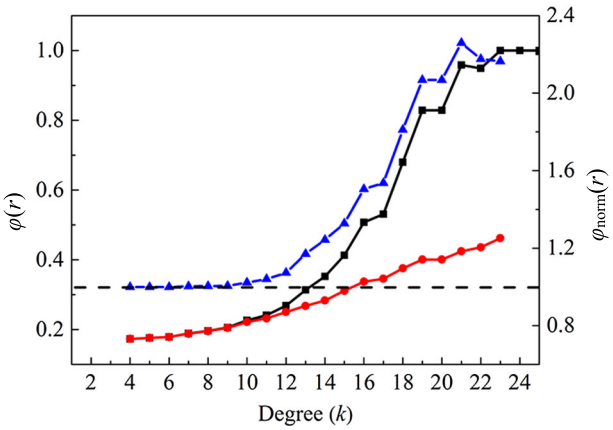

Fig. 4 The Rich Club coefficients of the brain functional network

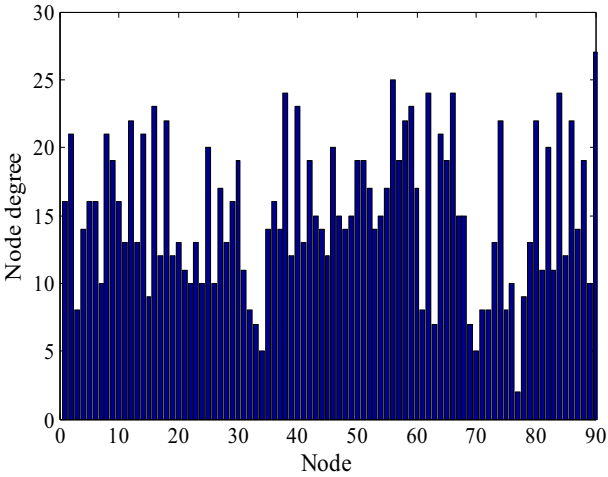

Fig. 5 Node degrees of brain functional network in stroke patients

above nodes play an important role in different time periods. Rich Club nodes in window *d* are: HIP.R, FFG.R, PoCG.R, IPL.R, ANG.R, HES.R, TPosup.R and ITG.R.

Node degree, clustering coefficient, and local efficiency are computed so as to understand the attribute difference of the nodes in different time periods. The nodes ANG.R and ITG.R are performed to explain this difference because they have the largest degrees of Rich Club in the brain functional network with entire fMRI time series. Figures 6, 7, and 8 show the three coefficients in different time windows, respectively, where *s* represents the entire fMRI time series, and is treated as a window.

Table 5 The node composition of Rich Club

Labels	Brain regions	Abbr (L: Left & R: Right)	Degree
2	Precental gyrus	PreCG.R	21
8	Middle frontal gyrus	MFG.R	21
12	Inferior frontal gyrus, opercular part	IFGoperc.R	23
14	Inferior frontal gyrus, triangular part	IFGtriang.R	21
16	Inferior frontal gyrus, orbital part	ORBinf.R	23
18	Rolandic operculum	ROL.R	22
38	Hippocampus	HIP.R	24
40	Parahippocampal gyrus	PHG.R	24
46	Cuneus	CUN.R	21
56	Fusiform gyrus	FFG.R	25
58	Postcentral gyrus	PoCG.R	23
62	Inferior parietal, but supramarginal and angular gyri	IPL.R	24
64	Supramarginal gyrus	SMG.R	22
66	Angular gyrus	ANG.R	26
74	Lenticular nucleus, putamen	PUT.R	22
80	Heschl gyrus	HES.R	23
82	Superior temporal gyrus	STG.R	25
84	Temporal pole: superior temporal gyrus	TPOsup.R	23
86	Middle temporal gyrus	MTG.R	23
88	Temporal pole: middle temporal gyrus	TPOmid.R	21
90	Inferior temporal gyrus	ITG.R	26

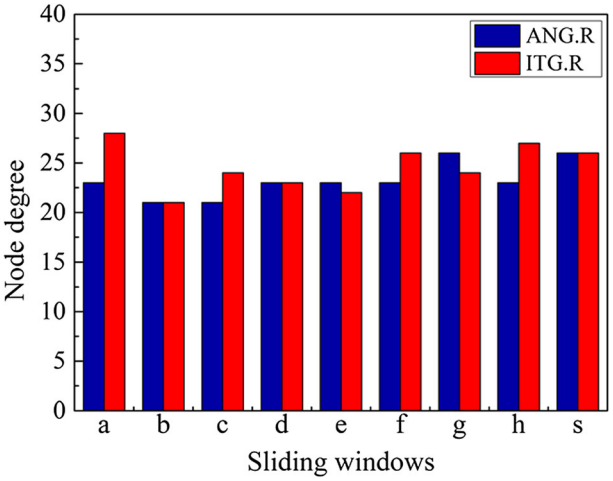

Fig. 6 Node degree in different time windows

In Rich Club node point of view, there are some distinguishable differences in node degree, clustering coefficient and efficiency of the nodes in different time periods. It suggests that the functional connectivity strength of nodes has certain differences at different time periods. Correspondingly, other indicators such as the betweenness and the information transfer rate are also constantly changing. Obviously, it is helpful to analyze the dynamic activities of the brain nerve by quantifying these indicators.

In summary, we effectively analyze Rich Club characteristics of dynamic brain functional networks in resting state. Dynamic brain functional networks are constructed to analyze the functional characteristics of Rich Club. Feeder connection and Local connection at different time periods are gained and the impact of various connections on Rich Club efficiency is examined by calculating the number of rich connections. The experimental results show that the number and types of nodes in the Rich Club at discrete time periods have changed in certain network densities. Nevertheless, some nodes are always Rich Club node at different

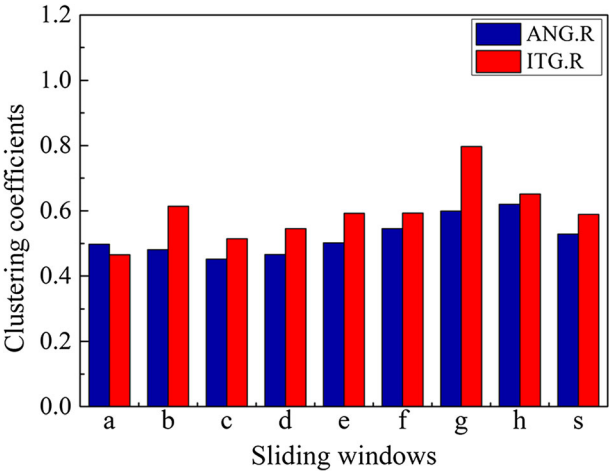

Fig. 7 Clustering coefficients in different time windows

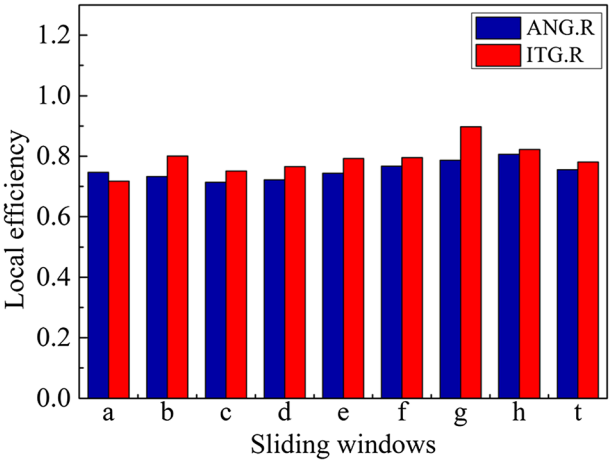

Fig. 8 Local efficiency in different time windows

time periods, and it indicates that these nodes are always play an important role for brain neural activity. It also found that Rich Club has a consistent distribution in the dynamic brain functional network at different time periods. Notably, the proposed method does not contain the investigation of different classifiers in deep CNN models for disease diagnose. Therefore, our future work will be focused on a feature selection mechanism based on Rich Club characteristics of the patients with stroke [20], Alzheimer's disease [50], and other diseases.

Acknowledgements The authors would like to thank the reviewers and the editors for their valuable comments and suggestions on improving this paper. This work is supported by the National Natural Science Foundation of China (No. 51307010), the Natural Science Foundation of Jiangsu Province and the University Natural Science Research Program of Jiangsu Province (No. 17KJB510003).

Authors' contributions ZJ and HW conceived of the study and contributed to the manuscript. SW contributed to the resting-state functional networks analysis. YC and LZ contributed to the fMRI experimental design and analysis. All authors read and approved the final manuscript.

Compliance with ethical standards

Conflict of interest We have no conflicts of interest to disclose with regard to the subject matter of this paper.

Publisher's note Springer Nature remains neutral with regard to jurisdictional claims in published maps and institutional affiliations.

References

1. Breakspear M (2017) Dynamic models of large-scale brain activity. Nat Neurosci 20(3):340–352
2. Calhoun VD, Miller R, Pearlson G, Adal T (2014) The chronnectome: time-varying connectivity networks as the next frontier in fMRI data discovery. Neuron 84(2):262–274
3. Chen XB, Zhang H, Gao YZ, Wee CY, Li G, Shen DG (2016) High-order resting-state functional connectivity network for MCI classification. Hum Brain Mapp 37(9):3282–3296
4. Chen XB, Zhang H, Lee SW, Shen DG (2017) Hierarchical high-order functional connectivity networks and selective feature fusion for MCI classification. Neuroinformatics 15(3):1–14

5. Colizza V, Flammini A, Serrano MA, Vespignani A (2006) Detecting rich-club ordering in complex networks. Nat Phys 2(2):110–115
6. Daianu M, Jahanshad N, Nir TM, Jack CR Jr, Weiner MW, Bernstein MA, Thompson PM (2015) Rich club analysis in the Alzheimer's disease connectome reveals a relatively undisturbed structural core network. Hum Brain Mapp 36(8):3087–3103
7. Damaraju E, Allen EA, Belger A, Ford JM, McEwen S, Mathalon DH, Mueller BA, Pearlson GD, Potkin SG, Preda A, Turner JA, Vaidya JG, van Erp TG, Calhoun VD (2014) Dynamic functional connectivity analysis reveals transient states of dysconnectivity in schizophrenia. NeuroImage: Clin 5(C):298–308
8. Echávarri C, Aalten P, Uylings H, Jacobs H, Visser P, Gronenschild E, Verhey F, Burgmans S (2011) Atrophy in the parahippocampal gyrus as an early biomarker of Alzheimer's disease. Brain Struct Funct 215(3–4):265–271
9. Geng YY, Liang RZ, Li WZ, Wang JB, Liang GY, Xu CH, Wang JY (2016) Learning convolutional neural network to maximize pos@ top performance measure. ESANN 2017 proceedings, European symposium on artificial neural networks, Computational intelligence and machine learning: 589–594
10. Geng YY, Zhang GH, Li WZ, Gu Y, Liang RZ, Liang GY, Wang JB, Wu YB, Patil N, Wang JY (2017) A novel image tag completion method based on convolutional neural transformation. Lect Notes Comput Sci 10614:539–546
11. Griffa A, Baumann PS, Thiran JP, Hagmann P (2013) Structural connectomics in brain diseases. Neuroimage 80(20):515–526
12. Guusje C, Kahn RS, De RMA, Wiepke C, van den Heuvel M (2014) Impaired Rich Club connectivity in unaffected siblings of schizophrenia patients. Schizophr Bull 40(2):438–448
13. Harrington DL, Rubinov M, Durgerian S, Mourany L, Reece C, Koenig K, Long JD, Paulsen JS (2015) Network topology and functional connectivity disturbances precede the onset of Huntington's disease. Brain 138(8):2332–2346
14. Jiao ZQ, Zou L, Cao Y, Qian N, Ma ZH (2014) Effective connectivity analysis of fMRI data based on network motifs. J Supercomput 67(3):809–819
15. Jiao ZQ, Wang H, Ma K (2016) The connectivity measurement in complex directed networks by motif structure. Int J Sensor Netw 21(3):197–204
16. Jiao ZQ, Ma K, Rong YL, Wang H, Zou L (2017) Adaptive synchronization in small-world networks with Lorenz chaotic oscillators. Int J Sensor Netw 24(2):90–97
17. Jiao ZQ, Ma K, Wang H, Zou L, Zhang YD (2017) Research on node properties of resting-state brain functional networks by using node activity and ALFF. Multimedia Tools Appl. https://doi.org/10.1007/s11042-017-5163-2
18. Jiao ZQ, Wang H, Ma K, Zou L, Xiang JB (2017) Directed connectivity of brain default networks using GCA and motif. Front Biosci 22(10):1634–1643
19. Jiao ZQ, Ma K, Wang H, Zou L, Xiang JB (2017) Functional connectivity analysis of brain default mode networks using Hamiltonian path. CNS Neurol Disord Drug Targets 16(1):44–50
20. Jiao ZQ, Wang H, Ma K, Zou L, Xiang JB, Wang SH (2017) Effective connectivity in the default network using granger causal analysis. J Med Imaging Health Inform 7(2):407–415
21. Latora V, Marchiori M (2001) Efficient behavior of small-world networks. Phys Rev Lett 87(19):198701
22. Li HJ, Li HY (2016) Scalably revealing the dynamics of soft community structure in complex networks. J Syst Sci Complex 29(4):1071–1088
23. Ma A, Mondragón RJ (2014) Rich-cores in networks. PLoS One 10(3):e0119678
24. Markett S, de Reus MA, Reuter M, Montag C, Weber B, Schoene-Bake JC (2017) Serotonin and the brain's Rich Club-association between molecular genetic variation on the TPH2 gene and the structural connectome. Cereb Cortex 27(3):2166–2174
25. Marusak HA, Calhoun VD, Brown S, Crespo LM, Sala-Hamrick K, Gotlib IH, Thomason ME (2016) Dynamic functional connectivity of neurocognitive networks in children. Hum Brain Mapp 38(1):97–108
26. Mccolgan P, Seunarine KK, Razi A, Cole JH, Gregory S, Durr A, Roos RAC, Stout JC, Landwehrmeyer B, Scahill RI, Clark CA, Rees G, Tabrizi SJ (2015) Selective vulnerability of Rich Club brain regions is an organizational principle of structural connectivity loss in Huntington's disease. Brain 138(11):3327–3344
27. Nguyen TT, Kovacevic S, Dev SI, Lu K, Liu TT, Eyler LT (2016) Dynamic functional connectivity in bipolar disorder is associated with executive function and processing speed: a preliminary study. Neuropsychology 31(1):73–83
28. Pasquale F, Penna S, Sporns O, Romani G, Corbetta M (2016) A dynamic core network and global efficiency in the resting human brain. Cereb Cortex 26(10):878–896
29. Poulin SP, Dautoff R, Morris JC, Barrett LF, Dickerson BC (2011) Alzheimer's disease neuroimaging initiative. Amygdala atrophy is prominent in early Alzheimer's disease and relates to symptom severity. Psychiatry Res 194(1):7–13

30. Power JD, Schlaggar BL, Lessov-Schlaggar CN, Petersen SE (2013) Evidence for hubs in human functional brain networks. Neuron 79(4):798–813
31. Ray S, Miller M, Karalunas S, Robertson C, Grayson DS, Cary RP, Hawkey E, Painter JG, Fombonne E, Nigg JT, Fair DA (2015) Structural and functional connectivity of the human brain in autism spectrum disorders and attention-deficit/hyperactivity disorder: a rich club organization study. Hum Brain Mapp 35(12):6032–6048
32. Rubinov M, Sporns O (2010) Complex network measures of brain connectivity: uses and interpretations. Neuroimage 52(3):1059–1069
33. Sheline YI, Raichle ME (2013) Resting state functional connectivity in preclinical Alzheimer's disease. Biol Psychiatry 74(5):340–347
34. Sporns O, Honey C, Kötter R (2007) Identification and classification of hubs in brain networks. PLoS One 2(10):1049–1062
35. Tobia MJ, Hayashi K, Ballard G, Gotlib IH, Waugh CE (2017) Dynamic functional connectivity and individual differences in emotions during social stress. Hum Brain Mapp 38(12):6185–6205
36. Tzourio-Mazoyer N, Landeau B, Papathanassiou D, Crivello F, Etard O, Delcroix N, Mazoyer B, Joliot M (2002) Automated anatomical labeling of activations in SPM using a macroscopic anatomical parcellation of the MNI MRI single-subject brain. NeuroImage 15(1):273–289
37. Van MDH, Sporns O (2011) Rich-club organization of the human connectome. J Neurosci 31(44):15775–15786
38. Wang JH, Zuo X, He Y (2010) Graph-based network analysis of resting-state functional MRI. Front Syst Neurosci 4(16):16
39. Wang X, Ren YS, Zhang WS (2017) Multi-task fused lasso metllod for constructing dynamic functional brain network of resting-state fMRI. J Image Graph 22(7):0978–0987
40. Wang SH, Du SD, Atangana A, Liu AJ, Lu ZY (2018) Application of stationary wavelet entropy in pathological brain detection. Multimedia Tools Appl 77(3):3701–3714
41. Wang SH, Phillips P, Sui Y, Liu B, Yang M, Cheng H (2018) Classification of Alzheimer's disease based on eight-layer convolutional neural network with leaky rectified linear unit and max pooling. J Med Syst 42(5):85
42. Wee CY, Yang S, Yap PT, Shen D (2016) Sparse temporally dynamic resting-state functional connectivity networks for early MCI identification. Brain Imaging Behav 10(2):342–356
43. Yang M, Zhang Y, Li JW, Zou L, Lu SY, Liu B, Yang JQ, Zhang YD (2016) Detection of left-sided and right-sided hearing loss via fractional Fourier transform. Entropy 18(5):194
44. Yao ZQ, Shang KK, Xu XK (2012) Fundamental statistics of weighted networks. J Univ Shanghai Sci Technol 34(1):18–26
45. Zhang YD, Wang SH (2015) Detection of Alzheimer's disease by displacement field and machine learning. Peerj 3(s1):e1251
46. Zhang YD, Dong ZC, Phillips P, Wang SH, Ji GL, Yang JQ, Yuan TF (2015) Detection of subjects and brain regions related to Alzheimer's disease using 3D MRI scans based on eigenbrain and machine learning. Front Comput Neurosci 9:66
47. Zhang YD, Wang SD, Phillips P, Dong ZC, Ji GL, Yang JQ (2015) Detection of Alzheimer's disease and mild cognitive impairment based on structural volumetric MR images using 3D-DWT and WTA-KSVM trained by PSOTVAC. Biomed Signal Process Control 21:58–73
48. Zhang YD, Chen XQ, Zhan TM, Jiao ZQ, Sun Y, Chen ZM, Yao Y, Fang LT, Lv YD, Wang SH (2016) Fractal dimension estimation for developing pathological brain detection system based on Minkowski-Bouligand method. IEEE Access 4:5937–5947
49. Zhang YD, Yang JQ, Yang JF, Liu AJ, Sun P (2016) A novel compressed sensing method for magnetic resonance imaging: exponential wavelet iterative shrinkage-thresholding algorithm with random shift. Int J Biomed Imaging 3:1–10
50. Zhang YD, Wang SH, Phillips P, Yang JQ, Yuan TF (2016) Three-dimensional eigenbrain for the detection of subjects and brain regions related with Alzheimer's disease. J Alzheimers Dis 50(4):1163–1179
51. Zhang YD, Yang M, Wang SH (2017) Two-level iterative compressed sensing for cardiovascular magnetic resonance imaging. J Am Coll Cardiol 70(16):C167
52. Zhang GH, Liang GY, Li WZ, Fang J, Wang JB, Geng YY, Wang JY (2017) Learning convolutional ranking-score function by query preference regularization. Lect Notes Comput Sci 10585:1–8
53. Zhang Y, Zhang H, Chen XB, Lee SW, Shen DG (2017) Hybrid high-order functional connectivity networks using resting-state functional MRI for mild cognitive impairment diagnosis. Sci Rep 7(1):6530
54. Zhou S, Mondragon RJ (2003) The rich-club phenomenon in the internet topology. IEEE Commun Lett 8(3):180–182
55. Zhou XX, Zhang YD, Ji GL, Yang JQ, Dong ZC, Wang SH, Zhang GS, Phillips P (2016) Detection of abnormal MR brains based on wavelet entropy and feature selection. IEEJ Trans Electr Electron Eng 11(3):364–373

Zhuqing Jiao is presently an Associate Professor at the School of Information Science and Engineering, Changzhou University, China. He received his Ph.D. from the School of IoT Engineering at Jiangnan University in 2011. His current projects are in the areas of intelligent computing, computer-aided diagnosis and brain network, etc.

Huan Wang is a Master's Degree Candidate at the School of Information Science and Engineering, Changzhou University, China. He received his Bachelor's degree in Changzhou University in 2015. His research interests include brain functional network.

Min Cai is also a Master's Degree Candidate at the School of Information Science and Engineering, Changzhou University, China. She received her Bachelor's degree from Southeast University Chengxian College, Nanjing, 2016. Her research interests encompass cognitive computing.

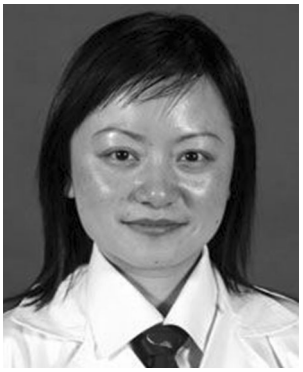

Yin Cao is a Chief Physician at the Department of Neurology, Changzhou Second People's Hospital Affiliated to Nanjing Medical University, China. She received her Master's degree in Nanjing Medical University in 2010. Her research interests focus on diagnosis and treatment of Neurology diseases.

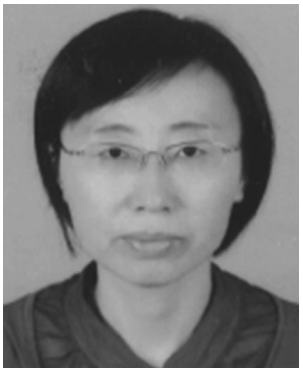

Ling Zou is a Professor at the School of Information Science and Engineering, Changzhou University, China. She received his Ph.D. from the School of Electrical Engineering at Zhejiang University in 2004. Her research interest is human-computer interaction, biomedical signal processing and pattern recognition.

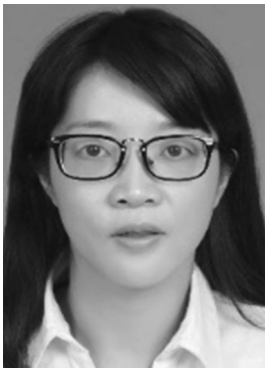

Shuihua Wang is currently a Visiting Researcher at the Department of Informatics, University of Leicester, UK. She received her Ph.D. from Nanjing University, in 2016. Her research interest is biomedical image processing and computer aided diagnosis.

Affiliations

Zhuqing Jiao[1] · Huan Wang[1] · Min Cai[1] · Yin Cao[2] · Ling Zou[1] · Shuihua Wang[3]

✉ Ling Zou
zouling@cczu.edu.cn

✉ Shuihua Wang
shuihuawang@ieee.org

[1] School of Information Science and Engineering, Changzhou University, Changzhou 213164, China

[2] Department of Neurology, Changzhou Second People's Hospital Affiliated to Nanjing Medical University, Changzhou 213003, China

[3] Department of Informatics, University of Leicester, University Road, Leicester LE1 7RH, UK